Translational Oncology
www.transonc.com

Volume 5 Number 4 August 2012 pp. 230–237 230

An Integrated Method for Reproducible and Accurate Image-Guided Stereotactic Cranial Irradiation of Brain Tumors Using the Small Animal Radiation Research Platform[1]

Brian C. Baumann, Joseph L. Benci, Phillip P. Santoiemma, Sanjay Chandrasekaran, Andrew B. Hollander, Gary D. Kao and Jay F. Dorsey

Department of Radiation Oncology and the Division of Radiobiology, Perelman School of Medicine at the University of Pennsylvania, Philadelphia, PA

Abstract

Preclinical studies of cranial radiation therapy (RT) using animal brain tumor models have been hampered by technical limitations in the delivery of clinically relevant RT. We established a bioimageable mouse model of glioblastoma multiforme (GBM) and an image-guided radiation delivery system that facilitated precise tumor localization and treatment and which closely resembled clinical RT. Our novel radiation system makes use of magnetic resonance imaging (MRI) and bioluminescent imaging (BLI) to define tumor volumes, computed tomographic (CT) imaging for accurate treatment planning, a novel mouse immobilization system, and precise treatments delivered with the Small Animal Radiation Research Platform. We demonstrated that, *in vivo*, BLI correlated well with MRI for defining tumor volumes. Our novel restraint system enhanced setup reproducibility and precision, was atraumatic, and minimized artifacts on CT imaging used for treatment planning. We confirmed precise radiation delivery through immunofluorescent analysis of the phosphorylation of histone H2AX in irradiated brains and brain tumors. Assays with an intravenous near-infrared fluorescent probe confirmed that radiation of orthografts increased disruption of the tumor blood-brain barrier (BBB). This integrated model system, which facilitated delivery of precise, reproducible, stereotactic cranial RT in mice and confirmed RT's resultant histologic and BBB changes, may aid future brain tumor research.

Translational Oncology (2012) 5, 230–237

Introduction

Glioblastoma multiforme (GBM) is a primary brain cancer with a median survival of only 14.6 months despite standard multimodality treatment with surgical resection, postoperative RT, and temozolomide chemotherapy [1]. New therapeutic approaches are urgently needed to improve patient survival and quality of life. The development of new treatment strategies is limited in part by the quality of preclinical animal models of GBM and by preclinical RT techniques that have lagged far behind current clinical practice.

Until recently, animal irradiation was typically conducted using fixed radiation sources applying a single radiation field. Sparing of normal tissue was usually achieved with lead shielding to cover the animal while

Address all correspondence to: Jay F. Dorsey, MD, PhD, Department of Radiation Oncology, Perelman Center for Advanced Medicine, TRC2W, 3400 Civic Center Blvd, Philadelphia, PA 19104. E-mail: JayD@uphs.upenn.edu

[1]The authors acknowledge the support of Dr Ann Kennedy and the grant submitted by Drs Cameron Koch and Costas Koumenis, which funded the purchase of the Small Animal Radiation Research Platform used in the experiments described in this article. B.C.B. was supported by the Radiation Biology training grant C5T32CA009677. J.L.B. was supported by the SUPERs grant 5 R25 CA140116-03. J.F.D. was supported by a Burroughs Wellcome Career Award for Medical Scientists (1006792). This work was supported by the National Institutes of Health (RC1 CA145075 and K08 NS076548-01). A patent application for the novel stereotactic mouse restrainer is in preparation.
Received 5 March 2012; Revised 23 May 2012; Accepted 24 May 2012

DOI 10.1593/tlo.12136

exposing the areas to be treated. The accuracy of dosimetric calculations was limited, and the ability to target a treatment volume precisely remained largely beyond the reach of these simple techniques. The recent development of three-dimensional conformal small animal microirradiator systems has been a major step forward [2–4]. One such system developed at Johns Hopkins University is the Small Animal Radiation Research Platform (SARRP), an image-guided x-ray microirradiator with an onboard high-resolution CT scanner that can deliver noncoplanar radiation to an anatomic target with precision [3].

We sought to establish an animal model system that more accurately reflects current clinical practice by coupling the SARRP's precise radiation delivery with imaging techniques that can accurately localize targets and then apply these sophisticated techniques to orthotopic, bioimageable GBM implants in mice that closely mimic the clinical characteristics of human GBM tumors. In this article, we describe our animal model for GBM and our RT techniques, including a novel CT-compatible immobilization system that we designed and constructed for focal brain irradiation that ensures day-to-day reproducibility without trauma to the animal. We further describe histologic and imaging techniques to verify the treatment accuracy of the delivered radiation, and the ensuing effects on disrupting the blood-brain barrier (BBB) of the targeted brain tumor.

Materials and Methods

All animal experiments were performed in accordance with Institutional Animal Care and Use Committee guidelines under the terms of an Institutional Animal Care and Use Committee–approved protocol.

Mouse Model of GBM

Labeling tumor cells to express firefly luciferase and green fluorescent protein. The human-derived GBM tumor cell line U251 was transduced with a lentiviral construct (pGreenFire; System Biosciences, Mountain View, CA) containing the firefly luciferase gene and the green fluorescent protein (GFP) gene under the control of a spleen focus-forming virus promoter. About 200,000 cells were plated and washed with phosphate-buffered saline (PBS). Thawed viral particles in 250 μl of Dulbecco modified Eagle medium were added to the cells. Cells were incubated for 72 hours. After transfection, supernatant with virus was collected and passed through a 22-nm filter. The filtered supernatant was used to infect the target U251 cells. The transduced U251 cells were sorted twice with flow cytometry to select the 1% of cells with the greatest fluorescence for propagation in culture and for implantation as xenograft tumors in nude mice.

Intracranial implantation of tumor cells. Nude athymic NCr mice (*nu/nu*) were weighed and premedicated 1 hour before intracranial implantation with a subcutaneous injection of 5 mg/kg of meloxicam in saline to control for postoperative pain and inflammation. The mice were anesthetized with an intraperitoneal injection of ketamine/xylazine at doses of 140 and 10 mg/kg, respectively. Once the anesthesia extinguished the mouse's response to light pinching of the rear foot, the mouse was immobilized in a stereotactic device (Stoelting Digital Just for Mice Stereotactic Instrument [Stoelting, Wood Dale, IL]; Figure 1*A*). The mouse's temperature was monitored with a rectal probe and maintained at 37°C with feedback control to a heating plate underneath the animal. An ophthalmic ointment was applied to prevent drying. Using aseptic technique, the top of the head was swabbed with betadine, and the skull was exposed through a 0.5-cm longitudinal scalp incision. Using the stereotactic armature, a small hole was drilled using the Foredom Microdrill (Foredom, Bethel, CT) with a 0.4-mm burr at a site 2 mm posterior and 1.5 mm lateral to the bregma in the right cerebral hemisphere (Figure 1*A*). Through this hole, a stereotactically guided syringe with a 30-gauge flat bevel needle delivered approximately 300,000 luciferase/GFP–expressing U251 human brain tumor cells in 6 μl of Dulbecco modified Eagle medium at a depth of 2.5 mm within the brain parenchyma at an injection rate of 0.5 μl/min using the Automated Injector Pump by Harvard Apparatus [5]. After injection, the needle was left in the brain for a period of 2 minutes and then slowly withdrawn. The incision was closed with bone wax, the skin was reapproximated with glue, and the animal was moved to a heated pad for postoperative recovery.

Bioluminescent imaging. Mice were imaged using the IVIS Lumina II (Caliper, Hopkinton, MA) bioluminescence imaging (BLI) system beginning 1 week after tumor injection. The mice were anesthetized by intraperitoneal injection with ketamine/xylazine (140:10 mg/kg) before receiving a subcutaneous injection of 60 μl of D-luciferin (50 mg/ml), which freely crosses the BBB [6]. Imaging through the IVIS system commenced 5 minutes after the luciferin injection and was repeated over a span of 30 minutes to determine the maximum luminescence intensity in photons/second, a surrogate marker for the size of the tumor. After image acquisition, a volume of interest was drawn around each tumor, and a background volume of interest was selected in an area free from tumor to generate a background-corrected bioluminescence flux value for each tumor at each given time point. The maximum background-corrected value for that tumor during the 30-minute imaging session was used as the maximum bioluminescent value. The bioluminescence of tumors was tracked over time using a measure termed *fold*, which was defined as follows: [current max BLI signal]/[initial pretreatment max BLI signal] [7,8]. IVIS imaging was repeated at least weekly to measure tumor size.

Multimodality Imaging to Localize Tumors

Magnetic resonance imaging. T2-weighted spin-echo *in vivo* magnetic resonance imaging (MRI) was performed to determine the size and anatomic location of the brain tumor for accurate targeting with RT. The mice were anesthetized with 1.0% to 1.5% isoflurane in oxygen administered at a flow rate of 1 L/min through a nose cone. The mouse was placed in a custom-built restrainer, and the restrainer was placed in a 20-mm radiofrequency coil (Cryogenic Preclinical 9.4-T Mouse Neuro Coil; m2m Imaging Corp, Cleveland, OH). An MR-compatible small animal monitoring system with a rectal fiber-optic temperature probe (SA Instruments, Stony Brook, NY) was used to record the animal's body temperature, which was maintained at 36.8°C by blowing warm air through the magnet bore. The mouse's respirations were monitored with a respiratory pillow. MRI was performed on a Varian 9.4-T 31-cm horizontal-bore MR spectrometer (Varian, Palo Alto, CA) equipped with a 21-cm ID gauss/cm and a 12-cm ID gauss/cm gradient tube and interfaced to a Varian Direct Drive console. A localizer scan was performed followed by a T2-weighted spin-echo scan with the following parameters: echo time = 2000 milliseconds, repetition time = 40 milliseconds, number of averages = 4, slice thickness = 0.5 mm, field of view = 20 × 20 mm, and matrix = 256 × 256 to generate high-resolution images. MR images were processed using ImageJ software (NIH Bethesda, MD) and Amira software (Visage Imaging, San Diego, CA). Amira was used to measure tumor dimensions

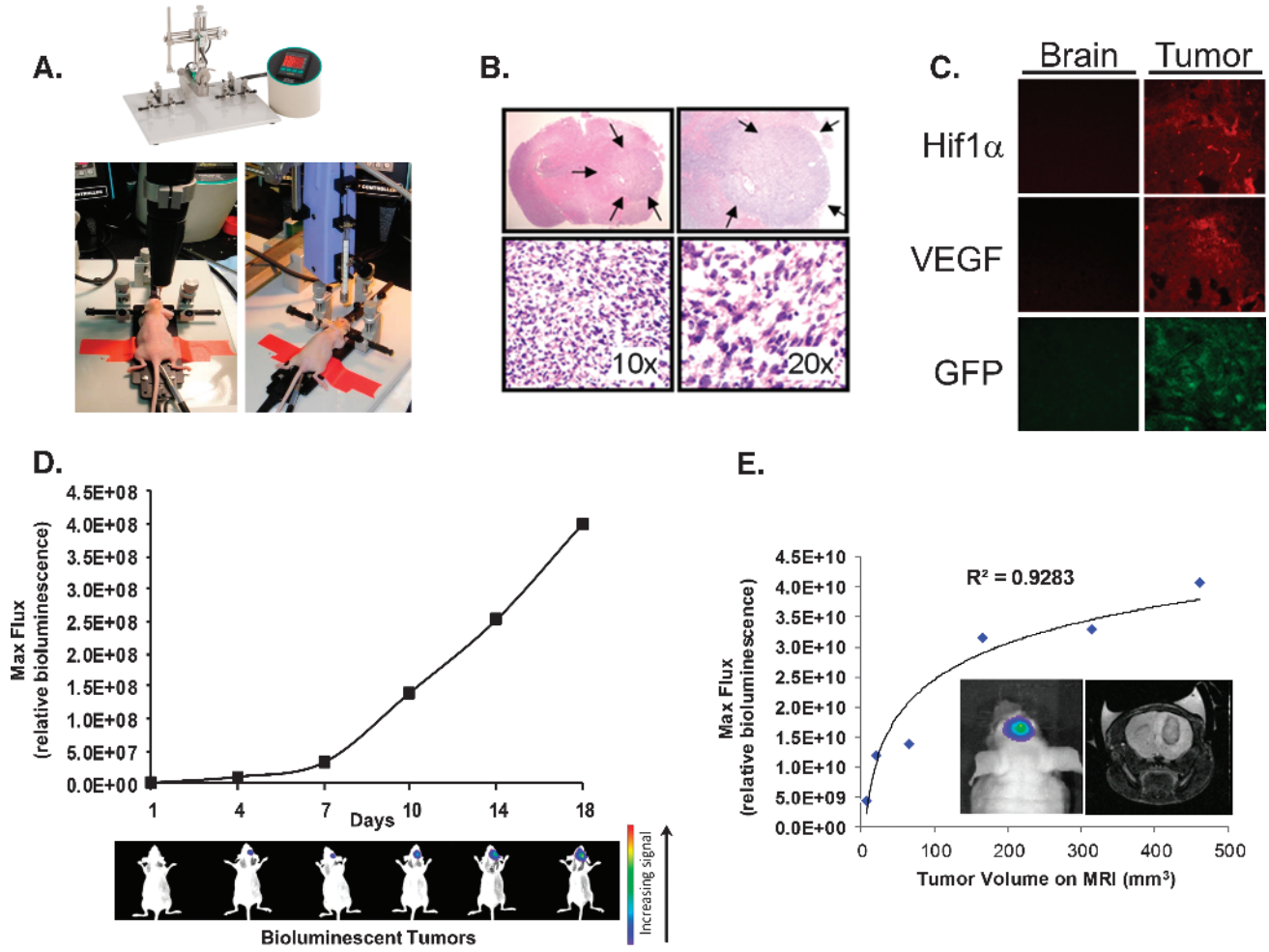

Figure 1. Establishing human-derived orthotopic GBM tumors in mice and subsequent imaging with bioluminescent and MR imaging. (A) Stereotactic implantation of GBM cells expressing GFP and luciferase into the brains of nude mice to create orthotopic tumors. (B) Hematoxylin/eosin staining of brains excised from mice shows the orthotopic tumor, designated within the arrows, under light microscopy at four different magnifications. (C) Orthotopic GBM tumors show robust expression of HIF-1α and VEGF. Normal brain (left column) or orthotopic brain tumor tissue (right column) were sectioned, fixed onto slides, and stained for HIF-1α (top) or VEGF (middle) protein expression. The bottom row shows expression of GFP. The immunofluorescent analyses were performed through the respective specific primary antibodies followed by red fluorescent protein (RFP)–labeled secondary antibodies to detect the specific signal. (D) BLI shows serial growth of the implanted tumors (representative mice shown during BLI on the specified day after initial implantation of tumor cells). Bioluminescence flux also reflects intracranial growth patterns. GBM cells expressing GFP and luciferase were stereotactically implanted, followed by *in vivo* serial BLI of the resultant brain tumors. BLI flux was defined as photons per second per squared centimeter, which reliably reflected intracranial growth patterns. (E) Bioluminescent imaging signal from tumors growing within the mouse correlate well with tumor volume measured after excision. *In vivo* BLI signal ("Bioluminescent Max Flux") was recorded for mice orthotopic brain tumors immediately before sacrifice. The tumors of each mouse were then excised, and the respective volume of each tumor was manually measured. The measured tumor volumes significantly correlate with BLI values ($R^2 = 0.9283$).

(Figure 2*A*), which were used to determine the collimator size and isocenter depth for a radiation portal that would adequately encompass the entire tumor while minimizing dose to adjacent normal tissues.

Bioluminescent imaging to confirm tumor targeting. Immediately before radiation, intracranial tumors were imaged using BLI as previously described to determine the anatomic location of maximum bioluminescent signal intensity by increasing the threshold of bioluminescent flux until only the brightest area of signal was evident as a few pixels (Figure 2*B*). This area was marked on the animal's scalp with a marker, and the animal was rescanned to confirm that the mark corresponded to the highest BLI signal intensity, which would be used to localize the isocenter for radiation portals.

RT stereotactic immobilization device. We designed a novel restraint system (Figure 2*C*) to optimize the delivery of focused radiation beams targeting the mouse's intracranial xenografts. All materials were selected so as to avoid interference with the onboard CT scanner on the SARRP irradiator. The restraining device consisted of a fiberglass base attached with plastic screws to the removable, fiberglass SARRP platform constructed by Xstrahl (Camberley, United Kingdom). Attached to the base of the restraint is a semicircular cradle made of the phenolic compound Garolite (McMaster-Carr, Chicago, IL), which supports the mouse and limits its movement. An adjustable-length bite bar constructed with Delrin (DuPont, Wilmington, DE) holds the animal's snout in position; this was hollowed out along its entire length to allow delivery of isoflurane anesthesia directly into the animal's mouth, obviating the need

for a nose cone that would partially obscure the animal's head and interfere with the placement and visualization of fiducial marker landmarks for radiation targeting. A fully adjustable ear bar system anchored the animal's head in position using Garolite-constructed ear bars. The height of each ear bar could be adjusted within a range of 1.2 cm and can then be screwed into place at the desired height on the polyvinyl chloride–constructed ear bar towers. The ear bars were then positioned within the ear canals using the appropriate degree of tension to immobilize the head in a level plane without causing trauma to the animal.

Use of fiducial markers to define and confirm radiation isocenters. Once the animal was positioned in the restrainer, a 1-mm-diameter nylon spherical fiducial marker was attached to the scalp with tissue glue at the spot of maximal BLI signal to serve as a guide for the selection of an isocenter during CT-guided treatment planning. Two additional nylon fiducial markers were placed lateral to the scalp fiducial markers in the same horizontal plane. These fiducial markers were spaced 3.5 cm apart within the field of view of the CT scanner, and the right fiducial marker was placed 1.4 cm from the scalp fiducial. These lateral fiducial markers appeared in the same coronal plane as the scalp fiducial marker on treatment planning CT scans (Figure 2*D*) and served as a check to ensure that the scalp fiducial marker was not displaced during setup.

Treatment planning and delivery of image-guided RT. High-resolution treatment planning CT scans were performed using the SARRP's onboard CT scanner linked to Pinnacle Treatment Planning software (Philips, Andover, MA). An isocenter was selected using the coronal, axial, and sagittal images produced by the CT scanner coupled with the fiducial markers placed to show the maximum BLI signal intensity (Figure 2*D*). The depth of the isocenter was previously determined based on the depth to the center of the tumor on the MRI scan. Once the isocenter was established, a treatment plan was generated, and the appropriately sized collimator for the radiation portal previously determined from the MRI was loaded onto the SARRP. The mouse's brain tumor was irradiated with a unidirectional superior-to-inferior

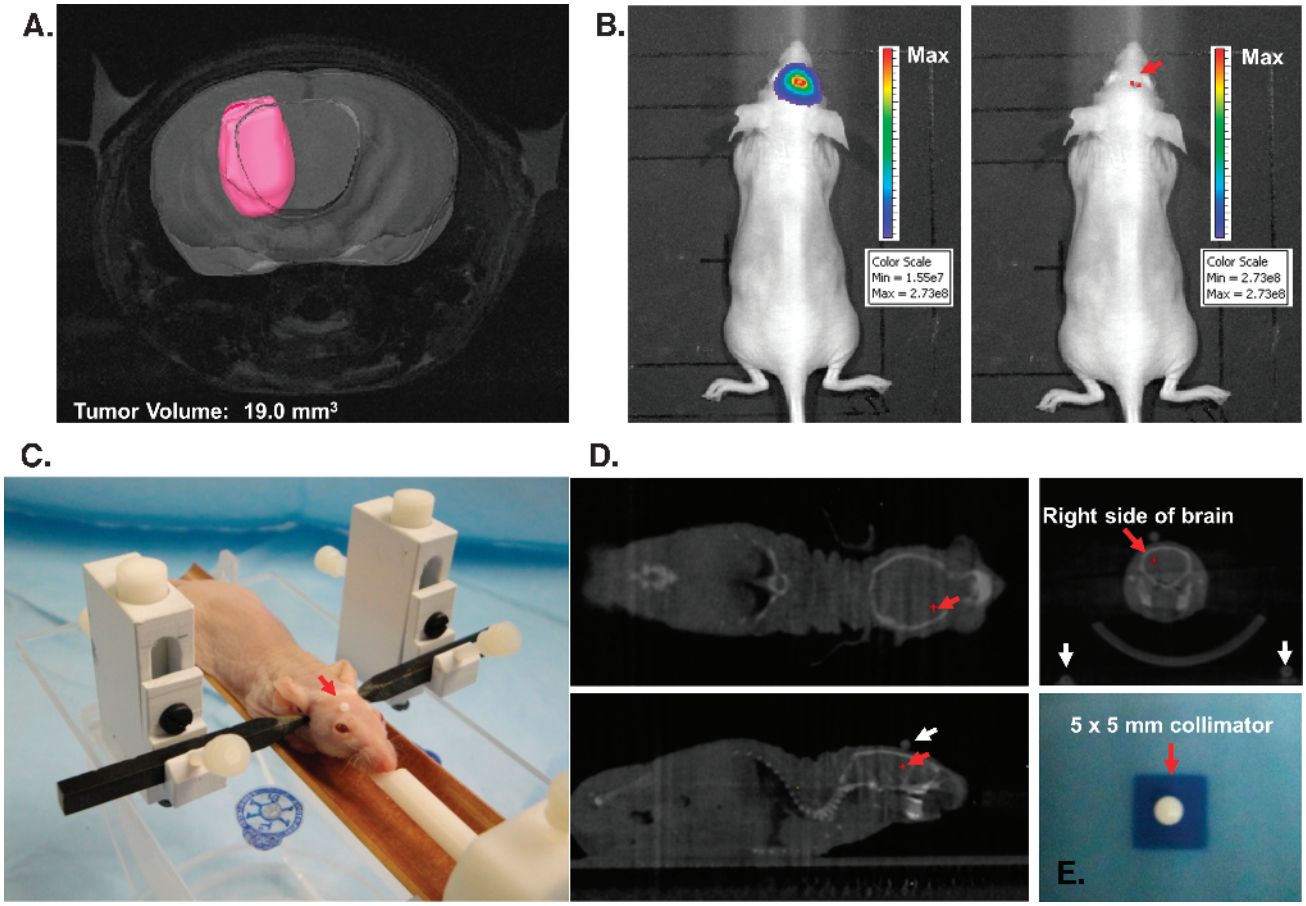

Figure 2. Image-guided stereotactic delivery of radiation to implanted tumors. (A) Spin-echo MRI of a mouse intracranial tumor using a 9.4-T MR spectrometer to determine the precise anatomic localization of the xenograft. The tumor volume was contoured in pink using the software package Amira. (B) Point of maximal bioluminescent signal for the tumor was determined (red arrow), and the spot was tattooed to aid in the setup of radiation treatment. (C) Anesthetized mouse secured in the home-built novel stereotactic restrainer. The point of maximal bioluminescent signal, identified previously, is covered by a fiducial marker (red arrow) to facilitate identification of the location on CT imaging for treatment planning. (D) Treatment planning CT scans showing the coronal, axial, and sagittal views of the brain. The small red crosses in each image indicate the selected isocenter. In the top right image, the coronal CT of the brain reveals three coplanar fiducial markers used to confirm proper setup for treatment (the scalp fiducial marker and two lateral fiducial markers on the restrainer seen at the bottom corners). (E) Irradiation of exposure film using the 5 × 5-mm collimator confirmed that the SARRP can deliver a collimated beam of radiation with very limited scatter. The irradiated field was centered within ±0.25 mm on its isocenter.

beam for a precalculated time interval to achieve the desired dose at a rate of 1.65 Gy/min using a 175-kV beam at 15 mA, with a 0.15-mm copper filter treating at 35-cm focus-to-skin distance.

Testing the accuracy of the CT-guided isocenter to predict the center of the irradiated field. A 1-mm nylon fiducial bead was affixed to Gafchromic EBT dosimetry exposure film (International Specialty Products, Wayne, NJ) and CT scanned using the SARRP. The center of the nylon fiducial marker was chosen as the isocenter for a 5 × 5-mm square collimator that was used to deliver 3 Gy to the film. The exposed area of film was evaluated to confirm that the center of the irradiated field corresponded to the marked isocenter (Figure 2*D*).

Phosphorylation of histone protein H2AX staining. To confirm precise localization of radiation to the intended target, immunohistochemical staining for a marker of radiation damage, γH2AX, was performed on *ex vivo* brain sections. One hour after radiation, the mouse's chest cavity was opened, and a continuous infusion of 1× PBS was pumped into the left ventricle through an 18-gauge needle. A separate incision in the right atrium allowed drainage of blood. The infusion continued until the circulating fluid was clear, and then 10% neutral buffered formalin was infused in the same manner. The animal was allowed to fix for 5 minutes before the whole brain was removed and postfixed in 10% formalin overnight. The brain was then placed in 30% sucrose for 3 days and transferred to isopentane until frozen (stored at −80°C). Tissue was sectioned coronally at 20-μm intervals with a cryostat (Microm HM 505 E; Microm, Walldorf, Germany) and stained with antibodies against phosphorylated γH2AX, a histone protein that is recruited to the site of double-strand breaks, as well as 4′,6-diamidino-2-phenylindole (DAPI) to visualize cell nuclei. These immunohistochemical sections were then visualized with fluorescence microscopy [9].

Assessing the effect of radiation on vascular permeability using near-infrared fluorescent imaging. To measure the effects of radiation on the vascular permeability of the tumor BBB, nude mice with U251-GFP-Luc intracranial GBM tumors with or without targeted cranial irradiation were imaged *in vivo* using the LI-COR Pearl near-infrared fluorescent imager after injection of near-infrared polyethylene glycol (PEG), a contrast agent designed to exploit the enhanced permeability and retention effect of leaky vascular endothelium. The radiated group had tumors that were evenly matched in BLI signal intensity. They received fractionated cranial irradiation (12 Gy in four fractions) 23 days after tumor implantation. BLI was repeated 30 days after radiation, and the BLI signal intensities of the tumors were used to select matched controls from a cohort of previously unirradiated mice with identically implanted intracranial tumors. Before fluorescent imaging, mice were injected through tail vein with 100 μl (1 nmol) of near-infrared PEG contrast agent (LI-COR's IRDye 800 CW PEG). *In vivo* fluorescent imaging was performed at intervals after injecting the contrast agent (at 30 minutes and at 2, 24, and 36 hours) followed by *ex vivo* imaging of the brain, liver, and blood 36 hours after injection of the contrast agent.

Results

U251 Glioblastoma Mouse Model

We used U251 cells for our studies because it is a human GBM cell line that, when implanted in mice, retains numerous characteristics frequently observed in human tumors [10]. To track the growth of these cells over time and to distinguish them from host tissues, the U251 cells were transduced to express genes for luciferase and green fluorescent protein (GFP) that enabled these cells to be readily detected through BLI as well as by *ex vivo* fluorescent microscopy.

We confirmed that these implanted tumors recapitulated many of the key features associated with glioblastoma, such as invasion of adjacent brain tissue, necrosis, regions of hypoxia with increased hypoxia-inducible factor (HIF-1α) expression, and increased vascular endothelial growth factor (VEGF; Figure 1*C*). The rapidly increasing signal over time on BLI revealed that these implants consistently demonstrated the high growth pattern expected with intracranial GBM (Figure 1*D*).

We previously confirmed *in vitro* that the intensity of the bioluminescent signal was directly proportional to the number of viable luciferase-expressing GBM cells [11]. In a pilot experiment using six mice, a logarithmic best-fit test showed a strong correlation ($R^2 = 0.928$) between bioluminescent signal intensity and tumor volume determined from *in vivo* MRI scans (Figure 1*E*). These studies established that our animal model of GBM recapitulated clinical features of human tumors, yet it was amenable to serial noninvasive BLI.

Image-Guided Stereotactic Delivery of Radiation to Implanted Tumors

A cohort of nude mice with U251-GFP-Luc intracranial tumor implants was imaged with BLI 18 days after implantation. BLI revealed an intense area of signal limited to the site of tumor implantation with an average maximum flux value of 1.30*e* + 09 photons/sec. Seven mice had their discrete point of maximal BLI signal intensity determined as described in the Materials and Methods section (Figure 2*B*) and were then scanned using a spin-echo MRI protocol on a 9.4-T horizontal-bore preclinical MR spectrometer to determine the precise anatomic localization of their xenografts (Figure 2*A*). The point of maximal BLI corresponded to the center of the tumor on MRI within ±0.5 mm in any direction where the average maximal distance from the center of the tumor to the tumor periphery was 1.7 mm and the average volume for these tumors was 26.1 mm^3.

Using Amira, we measured the dimensions of the tumor on coronal MRI sections in one mouse with a representative tumor burden on BLI (1.58*e* + 09 photons/sec) as 3.5 × 4.7 × 3 mm with a volume of 19.0 mm^3 (Figure 2*A*). On the basis of these dimensions, a 5 × 5-mm square collimator was selected to provide adequate coverage of the gross tumor volume with an appropriate clinical margin while sparing normal surrounding brain. The mouse's tumor was irradiated to 20 Gy in a single fraction on the SARRP using the restrainer and fiducial marker system described in the Materials and Methods section (Figure 2, *C* and *D*).

We had previously confirmed that the SARRP could deliver a collimated beam of radiation with very limited scatter. Irradiation of exposure film to 3 Gy using the 5 × 5-mm collimator resulted in a sharply marginated, homogeneous, square pattern of exposure with 5 × 5-mm dimensions that was centered within ±0.25 mm on its isocenter (Figure 2*E*).

After delivery of the 20-Gy dose, γH2AX staining of the mouse's brain showed a well-demarcated volume of positive γH2AX staining limited to the 5 × 5-mm radiation portal that successfully encompassed the entire tumor volume (Figure 3).

To confirm the accuracy of our system for stereotactic radiation treatment of mice brains, we irradiated the right hemisphere of a non–tumor-

bearing mouse brain to 20 Gy using a rectangular collimator (7 × 2 mm; Figure 3). The results of γH2AX staining on coronal brain sections showed a clearly demarcated 2-mm band of positive γH2AX staining that corresponded to the radiation portal. There was no evidence of radiation injury on either side of the 2-mm field.

These results confirmed that we could accurately define the tumor volume with our treatment planning process and could treat the entire tumor precisely with our technique while sparing adjacent normal tissue.

Evaluating the Novel Stereotactic SARRP Immobilization Device

To confirm that our novel restraint does not introduce signal artifact to the CT scanner, a CT scan of a mouse obtained with our stereotactic cranial SARRP restrainer was compared to a CT scan of the same mouse obtained with the standard restraint. The stereotactic brain restraint introduced only minimal additional artifact, which did not affect image resolution on the CT scan.

The novel stereotactic restraint resulted in no evidence of trauma to the mouth or ear canals of animals who were placed in the restraint for up to 50 minutes, equivalent to the time required to CT scan a mouse in the treatment position and deliver 60 to 70 Gy in a single dose—doses that would exceed the maximum clinically relevant dose for brain irradiation. The animals showed no ill effects from the restraint once they recovered from the anesthesia.

Targeted Radiation Results in Increased Permeability of the Tumor BBB

Nude mice harboring orthotopic U251-GFP-Luciferase intracranial GBM tumors evenly matched based on tumor bioluminescent signal intensity were treated with 12 Gy in four fractions. BLI was repeated 30 days later, and the BLI signal intensities were used to select tumor-matched controls from a cohort of untreated mice with implanted intracranial tumors. Mice in both groups were then injected with a near-infrared labeled PEG contrast imaging agent. To serve as additional controls, two separate cohorts of previously unirradiated nude mice without tumors were injected with an equal volume of either the near-infrared dye or PBS.

In vivo fluorescent imaging of the brains at 30 minutes and 2, 24, and 36 hours after injection of the near-infrared dye revealed increased signal in the irradiated tumors compared with the unirradiated tumors at all time points (Figure 4). At 24 hours after injection, the irradiated tumor group demonstrated a 1247% increase in the background-corrected fluorescent signal compared with the mock-irradiated group with tumor implants. As expected, mice treated with PBS alone had no increased fluorescent signal in their brains. We confirmed that the

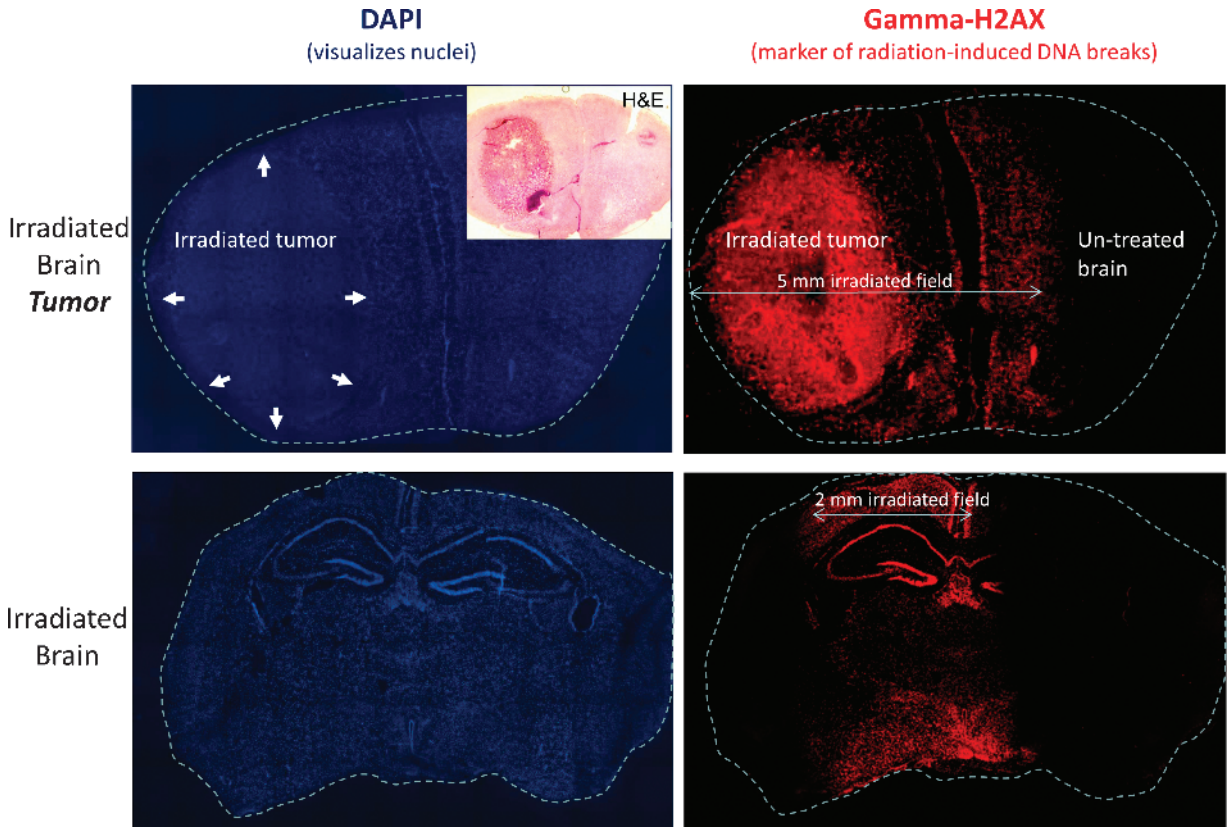

Figure 3. γH2AX staining of irradiated brain tissue confirms accurate delivery of stereotactic brain irradiation. Top row shows fluorescent microscopy images of coronal brain sections from a mouse with an intracranial (forebrain) tumor (marked with arrows) killed 2 hours after focal RT to 20 Gy in a single fraction using a 5 × 5-mm collimator, followed by staining for DAPI to visualize cell nuclei (left) and γH2AX to visualize radiation-induced unrepaired double-strand breaks (right). γH2AX staining confirms the precise targeting of the tumor using the described technique. The bottom row shows DAPI and γH2AX staining performed on coronal midbrain sections of a mouse without intracranial tumor killed 2 hours after focal RT to 20 Gy × 1 using a 7 × 2-mm collimator with the long axis parallel to the animal's spine.

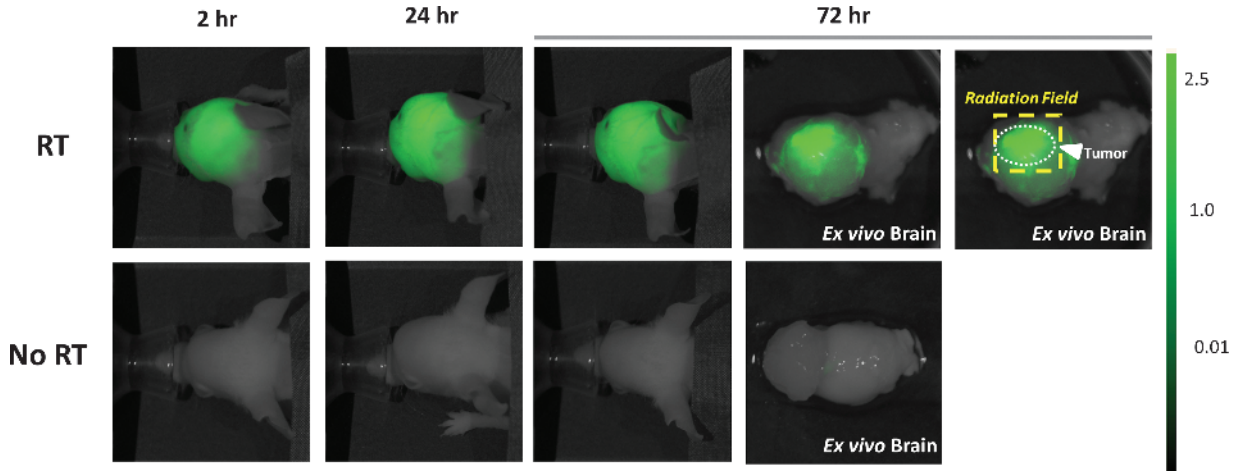

Figure 4. Targeted cranial RT for GBM orthografts is associated with increased extravasation of a near-infrared pegylated fluorescent probe, thus indicating disruption of the tumor BBB. Mice with intracranial tumors of comparable sizes (confirmed by tumor BLI signal) were irradiated through the SARRP ("RT," 12 Gy in four daily fractions) or mock irradiated ("No RT"). After completion of RT, mice were injected through the tail vein with LI-COR pegylated Near IR Dye. Serial *in vivo* fluorescent imaging revealed significantly increased fluorescent signal in the irradiated brain tumors at all time points, indicating increased BBB disruption induced by the focused radiation delivered. The group of three panels on the right (each labeled "Brain") shows the tumor-containing irradiated (top) or mock-irradiated (bottom) brains imaged after removal from the mouse ("*ex vivo* imaging"). The far right image confirms that increased BBB disruption within the brain tumor corresponded to the RT field. The dashed box delineates the RT field, within which extravasation of near-infrared fluorescent probe was maximal.

increased fluorescent signal localized to the brain tumors rather than to the surrounding normal brain tissue by *ex vivo* imaging of the harvested brains at 36 hours after injection. A comparison of the fluorescent signal from the extracted blood and *ex vivo* livers of all the mice given the near-infrared contrast agent revealed comparable signal intensities, suggesting that the different experimental results between treatment groups could not be ascribed to variations in the vascular concentration of the near-infrared contrast agent.

Interestingly, fluorescent signal from the mock-irradiated brain tumors was significantly greater ($P < .05$) than the signal from the normal brains of non–tumor-bearing control mice given the PEG contrast, suggesting that the presence of the implanted tumor resulted in some baseline degree of increased permeability of the tumor BBB that facilitated some extravasation of the contrast agent not observed in the normal mouse brain with an intact BBB.

The finding that both the *in vivo* and the *ex vivo* fluorescent signals of the RT-treated tumors were higher than those of the mock-irradiated tumors is consistent with the hypothesis that radiation leads to increased disruption of the tumor BBB resulting in increased extravasation of the contrast agent into the tumor.

Discussion

RT is a standard treatment for GBM as well as other brain and head and neck cancers. Until the development of commercially available small animal image-guided microirradiators like the SARRP, preclinical research in these disease sites was limited by small animal radiation techniques that lagged decades behind current clinical practice in the precise targeting of tumor volumes and the sparing of normal tissue [2,3]. Previously, only superficial tumors could be targeted with any degree of precision using crude lead blocking to shield the surrounding normal tissue. The development of the SARRP has opened up new avenues for preclinical RT research in these disease sites. The novel stereotactic head restraint and fiducial marker targeting techniques that we describe in this article offer an improvement on this technology, with potential applications not only for preclinical brain irradiation studies but also for studies involving any disease sites of the head and neck.

The SARRP's onboard CT scanner is limited in its ability to resolve intracranial tumors for targeting purposes. While the bony anatomy of the skull is well defined, allowing for easy identification of landmarks, the xenografts themselves are not well demarcated (Figure 2*D*). Use of a contrast agent can somewhat improve delineation of tumors, but our early experimentation with this technique has so far been unsatisfying. To supplement the limitations of the onboard CT scanner to visualize brain tumors, we believe it is valuable to use MRI scans with long echo time/long repetition time using thin slices to determine the tumor's location and dimensions for accurate targeting of the tumor.

While MRI is very good at defining tumor location and dimensions, the absence of treatment planning software that allows CT/MRI fusion somewhat limits the utility of MRI. BLI, although it cannot characterize the tumor's dimensions with the accuracy of MRI, is useful because the area of maximal BLI, which can be readily identified and marked on the animal in real time, is a very good surrogate marker for the center of the tumor as defined by MRI as we have demonstrated in our experiments. Placement of a fiducial marker over the area of maximal BLI signal can serve to confirm the location of the appropriate isocenter immediately before delivering radiation treatments using an appropriately sized collimator selected on the basis of the pretreatment MRI. The development of an onboard bioluminescent imager for real-time imaging when using the SARRP would greatly improve the efficiency of treatment planning, tumor targeting, and treatment setup by obviating the need to place fiducial markers on the scalp corresponding to the area of highest BLI signal.

As an illustration of the many potential applications of our SARRP-based, image-guided RT delivery techniques using our mouse model

of GBM, we performed a pilot study measuring the effect of stereotactic cranial RT to disrupt the GBM tumor BBB. Several preclinical and clinical studies have demonstrated that RT can cause focal disruption of the tumor BBB [12,13]. In our GBM mouse model, we previously confirmed that cranial RT effectively disrupted the GBM tumor BBB by showing that RT resulted in significantly greater IgG extravasation into tumors compared with unirradiated tumors or irradiated normal brain tissue. The effects were durable, with increased extravasation of IgG in the tumor still detectable by 35 days after RT [11]. Using *in vivo* near-infrared fluorescent imaging to assess endothelial permeability, we found that focal radiation of the tumor resulted in significantly more extravasation of pegylated near-infrared contrast agent into the tumor compared with unirradiated control tumors of equal size, a finding that was confirmed on *ex vivo* fluorescent imaging. This finding has implications for the use of targeted radiation to enhance delivery of cytotoxic agents that currently do not cross the tumor BBB in sufficient concentration to produce a therapeutic effect. To our knowledge, this pilot study is the first to use near-infrared *in vivo* imaging using a pegylated fluorescent probe to assay tumor BBB permeability in response to a treatment intervention. We think this technique may be a promising avenue for additional research and validation because *in vivo* fluorescent imaging using pegylated contrast agents is more cost-effective, is more rapid, and requires less expertise than do preclinical perfusion MRI studies such as dynamic contrast-enhanced MRI. A major limitation to the use of the *in vivo* fluorescent probe technique is that repeat injections of the fluorescent probe cannot be performed at less than 10-day intervals because of the long half-life of the agent in the circulation.

Our method of stereotactic irradiation of brain tumors applied to our animal model system of GBM represents an improvement in the ability of investigators to deliver precise radiation to carefully defined targets in preclinical experiments. Future advances in the technology of small animal microirradiator imaging and treatment planning, including the ability not only to define an isocenter but also to contour tumor volumes accurately using onboard imaging, will result in further improvements. The future of clinically relevant preclinical irradiation studies has never looked brighter.

Acknowledgments

The authors thank the helpful guidance and comments of John Wong (Johns Hopkins School of Medicine). The authors also thank Allen Bonner who helped design and build the novel stereotactic restrainer system; Cameron Koch, Xiangsheng Xu, Tim Jenkins, Lee Shuman, Christina Chapman, and Sara Davis for expert assistance; Steve Hahn whose invaluable encouragement and support helped make this research possible; the University of Pennsylvania Nano-Bio Interface Center and Dennis Discher for encouragement and helpful comments; and the Small Animal Imaging Facility at the University of Pennsylvania for usage of their MRI and Optical/Bioluminescence Core Facilities.

References

[1] Stupp R, Mason WP, van den Bent MJ, Weller M, Fisher B, Taphoorn MJ, Belanger K, Brandes AA, Marosi C, Bogdahn U, et al. (2005). Radiotherapy plus concomitant and adjuvant temozolomide for glioblastoma. *N Engl J Med* **352**, 987–996.

[2] Zhou H, Rodriguez M, van den Haak F, Nelson G, Jogani R, Xu J, Zhu X, Xian Y, Tran PT, Felsher DW, et al. (2010). Development of a micro–computed tomography–based image-guided conformal radiotherapy system for small animals. *Int J Radiat Oncol Biol Phys* **78**, 297–305.

[3] Wong J, Armour E, Kazanzides P, Iordachita I, Tryggestad E, Deng H, Matinfar M, Kennedy C, Liu Z, Chan T, et al. (2008). High-resolution, small animal radiation research platform with x-ray tomographic guidance capabilities. *Int J Radiat Oncol Biol Phys* **71**, 1591–1599.

[4] Stojadinovic S, Low DA, Hope AJ, Vicic M, Deasy JO, Cui J, Khullar D, Parikh PJ, Malinowski KT, Izaguirre EW, et al. (2007). MicroRT—small animal conformal irradiator. *Med Phys* **34**, 4706–4716.

[5] Baumann BC, Dorsey JF, Benci JL, Joh DY, and Kao GD (2012). Stereotactic intracranial implantation and *in vivo* bioluminescent imaging of tumor xenografts in a mouse model system of glioblastoma multiforme. *J Vis Exp*, In press.

[6] Lee KH, Byun SS, Paik JY, Lee SY, Song SH, Choe YS, and Kim BT (2003). Cell uptake and tissue distribution of radioiodine labelled D-luciferin: implications for luciferase based gene imaging. *Nucl Med Commun* **24**, 1003–1009.

[7] Hawes JJ and Reilly KM (2010). Bioluminescent approaches for measuring tumor growth in a mouse model of neurofibromatosis. *Toxicol Pathol* **38**, 123–130.

[8] Prasad G, Sottero T, Yang X, Mueller S, James CD, Weiss WA, Polley MY, Ozawa T, Berger MS, Aftab DT, et al. (2011). Inhibition of PI3K/mTOR pathways in glioblastoma and implications for combination therapy with temozolomide. *Neuro Oncol* **13**, 384–392.

[9] Rogakou EP, Pilch DR, Orr AH, Ivanova VS, and Bonner WM (1998). DNA double-stranded breaks induce histone H2AX phosphorylation on serine 139. *J Biol Chem* **273**, 5858–5868.

[10] Candolfi M, Curtin JF, Nichols WS, Muhammad AG, King GD, Pluhar GE, McNiel EA, Ohlfest JR, Freese AB, Moore PF, et al. (2007). Intracranial glioblastoma models in preclinical neuro-oncology: neuropathological characterization and tumor progression. *J Neurooncol* **85**, 133–148.

[11] Baumann BC, Dorsey JF, Xu X, Harada T, Chapman C, Benci J, Jaiswal S, Mahmud A, Discher DE, and Kao GD (2011). "Breaking through the tumor BBB": enhancing the efficacy of nanobiopolymer therapeutics against intracranial tumors with targeted radiation therapy [abstract]. *Int J Radiat Oncol Biol Phys* **81**, S145–S146.

[12] Lemasson B, Serduc R, Maisin C, Bouchet A, Coquery N, Robert P, Le Duc G, Tropres I, Remy C, and Barbier EL (2010). Monitoring blood-brain barrier status in a rat model of glioma receiving therapy: dual injection of low-molecular-weight and macromolecular MR contrast media. *Radiology* **257**, 342–352.

[13] Cao Y, Tsien CI, Shen Z, Tatro DS, Ten Haken R, Kessler ML, Chenevert TL, and Lawrence TS (2005). Use of magnetic resonance imaging to assess blood-brain/blood-glioma barrier opening during conformal radiotherapy. *J Clin Oncol* **23**, 4127–4136.